Article:

Bennett, J, Bell, AJ orcid.org/0000-0002-2061-3862, Stevenson, TJ et al. (1 more author) (2013) Tailoring the structure and piezoelectric properties of BiFeO3-(K0.5Bi0.5)TiO3-PbTiO3 ceramics for high temperature applications. Applied Physics Letters, 103 (15). 152901. ISSN 0003-6951

https://doi.org/10.1063/1.4824652

APPLIED PHYSICS LETTERS **103**, 152901 (2013)

Tailoring the structure and piezoelectric properties of $BiFeO_3$-$(K_{0.5}Bi_{0.5})TiO_3$–$PbTiO_3$ ceramics for high temperature applications

J. Bennett,[a] A. J. Bell, T. J. Stevenson, and T. P. Comyn
Institute for Materials Research, School of Process, Environmental and Materials Engineering, University of Leeds, Leeds, LS2 9JT, United Kingdom

(Received 3 September 2013; accepted 20 September 2013; published online 7 October 2013)

There is a growing requirement for piezoelectric materials and systems which can operate in extreme environments, for example, oil & gas, and aerospace. Here, we present the high temperature $BiFeO_3$-$K_{0.5}Bi_{0.5}TiO_3$-$PbTiO_3$ (BF-KBT-PT) polycrystalline perovskite system. X-ray diffraction, impedance analysis, and Berlincourt measurements reveal a large region of phase coexistence, which can be tailored to optimise performance; Tc and the tetragonal spontaneous strain correlate strongly with the $PbTiO_3$ concentration. The highest temperature composition has a d_{33} of 140 pmV^{-1} with a $T_c = 542\,°C$, occupying previously unchartered territory on the classical d_{33}–T_C plot. © *2013 AIP Publishing LLC*. [http://dx.doi.org/10.1063/1.4824652]

There is a technological demand for piezoelectric ceramics in actuators, sensors, and transducers with operating temperatures far greater than those of the ubiquitous lead zirconate titanate (PZT) ceramic.[1–4] PZT has a ferroelectric-paraelectric phase transition temperature, T_C, at 386 °C but is limited to operating at temperatures far below this, where its piezoelectric properties diminish.[5] The T_C in commercially used PZT ceramics is often estimated as lying between 250 °C and 350 °C.[6] The enhanced electromechanical properties experienced in PZT are due to the morphotropic phase boundary (MPB) that exists between $PbZrO_3$-rich rhombohedral and the $PbTiO_3$-rich tetragonal phases.[7] This MPB leads to a "softening" of the lattice and an increased number of possible polarizable directions due to the differing symmetries of each phase.

A higher T_C is often at the expense of piezoelectric properties,[8] an almost exclusive exception being $BiScO_3$-$PbTiO_3$ (BSPT) which is a promising alternative to PZT due to its excellent electrical properties and a T_C of 460 °C.[4,9] However, scandium is prohibitively expensive for widespread commercialisation.[10] After the discovery of BSPT, a wide range of systems were explored belonging to the $Bi(Me^{3+})O_3$-$PbTiO_3$ family, including Yb, Ga, and In, all with limited success.[4] The exhaustion of possible binary systems has led to the recent development of $PbTiO_3$ based ternary and pseudo-quarternary systems.[11–15] Other high temperature alternatives include non-perovskite structures such as; lead-niobate ($PbNbO_6$) which has a tungsten-bronze structure, bismuth titanate ($Bi_4Ti_3O_{12}$) which belongs to the bismuth structure layer ferroelectrics family and lithium niobate ($LiNbO_3$) which has a corundum structure, although these all offer relatively low piezoelectric coefficients (<85 pm/V).[1]

$xBiFeO_3$-$(1-x)PbTiO_3$ (BFPT) exhibits a MPB at $x = 0.7$, although this has been subject to much debate since its discovery, largely due to the sample form and techniques that have been used.[16] At $x = 0.7$, ferroelectricity remains up to 632 °C,[17] this is flanked by a broad mixed symmetry region (MSR) of R3c and P4mm perovskite phases between $0.4 < x < 0.7$. At the MPB the c/a ratio of the unclamped tetragonal phase is 1.18, in sintered ceramics this results in large internal stresses and as a relief mechanism the partial transformation of the tetragonal phase into the rhombohedral phase occurs, leading to the wide mixed symmetry region.[18] The consequence of the large c/a ratio at the MPB is the markedly high coercive field, E_C, and large electric fields are required to pole the materials.[19] The extrinsic contribution to the piezoelectric effect is small and is proposed to be due to low ferroelastic domain wall mobility.[20]

The $xBiFeO_3$-$(1-x)(K_{0.5}Bi_{0.5})TiO_3$ (BF-KBT) system has recently been reported,[21–25] as with many lead-free materials a number of difficulties were experienced during fabrication and densification using conventional sintering techniques. The $BiFeO_3$ rich compositions, where $x < 0.7$ belong to the rhombohedral R3c phase as determined using laboratory X-rays and neutron diffraction.[26] Morozov and Matsuo determined the presence of a MPB at $x = 0.6$ between the polar rhombohedral R3c phase and a psuedocubic phase which exists over a large compositional space between $0.25 < x < 0.6$. The large electric-field induced strains reported in BF-KBT are proposed to be due to the presence of polar nano-regions (PNRs) that are easily switched by an applied electric field;[23,24] however, the PNRs return to a random order upon removal of the field and, hence, the electromechanical properties are dominated by electrostriction. The current work presented here endeavours to demonstrate and interpret the electrical and structural properties of the $(1-x-y)BiFeO_3$-$x(K_{0.5}Bi_{0.5})TiO_3$-$_yPbTiO_3$ (BF-KBT-PT hereafter) system which has been shown to high piezoelectric strains.[27]

Ceramic powders of the BF-KBT-PT ternary system were prepared by conventional solid-state synthesis. Stoichiometric quantities of the starting reagents were mixed using a high energy attrition mill (Willy A. Bachofen, Basel, Switzerland) for 30 min with stabilized yttria stabilized zirconia balls in isopropyl alcohol, followed by drying and sieving. The powders

---

[a] pm07jb@leeds.ac.uk

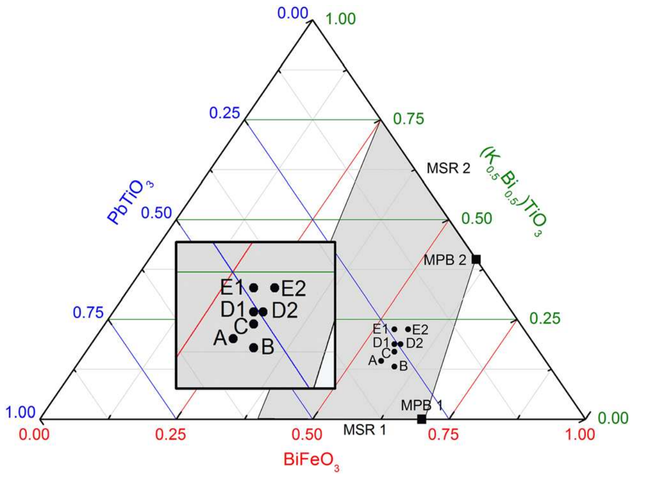

FIG. 1. The phase diagram of the BF-KBT-PT ternary system. MPB 1 and MPB 2 correspond to the BF-KBT, see Refs. 22 and 25, and BFPT, see Ref. 16, systems, respectively. MSR 1 and MSR 2 refer to broad mixed phase regions, MSR 1 is a coexistence of R3c and P4mm phases, see Ref. 18, while MSR 2 is pseudo-cubic, see Ref. 23.

were calcined at 800 °C for 4 h in covered crucibles. After calcination binder was added and the powders were pressed into pellets and sintered between 1050 °C–1065 °C. The compositions prepared are shown graphically in Figure 1 and tabulated in Table I. A wider examination of compositions belonging to this system has been undertaken, although not presented, and the compositions discussed in this contribution were chosen as they lie near to the MPB, as determined by XRD.

X-ray diffraction (Phillips X'Pert MPD, Almelo, The Netherlands) was used to identify the crystal structure of each composition. Room temperature X-ray diffraction (XRD) scans in the range $18° < 2\theta < 60°$ were used. This was undertaken on crushed and annealed powders in order to alleviate the influence of surface effects such as texture and stress.[28] Quantitative analysis of diffraction patterns was completed using PANalytical X'Pert HighScore Plus software.

In order to determine the ferroelectric T_C, relative permittivity was measured at 1 kHz–100 kHz as a function of temperature using an Agilent 4192A, with a non-inductively wound furnace. The T_C was determined from the maximum in permittivity upon cooling (at 3 °C/min) on unpoled samples.

The T_C in conventional lead-containing ceramics is usually regarded as a significant figure of merit when characterising piezoceramics, however, certain classes of materials, notably $(Bi_{1/2}Na_{1/2})TiO_3$-based ceramics lose their piezoelectric properties at temperatures far below the temperature of maximum of permittivity, this is termed the depolarization temperature, T_d.[6] Anton *et al.* discussed several methods of determining this figure in accordance with its definition, the resonance method was carried out following IEEE standard,[29] it was concluded that the resonance method was viable and previous studies have also used this technique.[30] An Agilent 4292a impedance analyser was used to observe resonance and anti-resonance peaks which were subsequently characterized using the Piezoelectric Resonance Analysis Program (PRAP) (TASI Technical Software, Kingston, Canada) in order to obtain the d_{31} and planar coupling coefficient, k_p, as a function of temperature from disc geometries. The samples were held at the measurement temperature for 10 min to allow for thermal stabilization. The poling conditions (electric field and temperature) were optimised for the various compositions, and varied between 6–7 kV/mm and 75–100 °C The poling time was held constant at 10 min, after this the samples were removed from the hot oil.

XRD analysis revealed the perovskite structure was formed with no discernible secondary phases (Fig. 2), the concentrations of KBT discussed here were fully soluble. Although not presented, peak broadening was much reduced in annealed crushed powders compared to bulk ceramics. Analysis of the diffraction patterns found that the compositions demonstrate peak splitting across all reflections, indicative of a phase co-existence. This is clear from the {200} reflection (Fig. 2(b)). Tetragonal materials exhibit splitting in the {200} family while rhombohedral materials do not. The broad (002) tetragonal peak can be observed at 43.75° for composition A. The reduction in the intensity and increase in the angle of the (002) peak is commensurate with a decrease in lead-titanate content, and can be seen to manifest as a broad shoulder in composition D2 at 44.92° and appears to be similar to those observed in the pseudo-cubic region in the BF-KBT system. The lack of substantial splitting across the {111} family confirms that the lattice distortion of the rhombohedral phase is very small, subsequently the tetragonal distortion would be expected to govern the

TABLE I. Summary of key structural and electrical properties in BF-KBT-PT, BSPT, and PZT ceramics.

Composition	A	B	C	D1	D2	E1	E2	PZT	BSPT
$(1\text{-}x\text{-}y)BiFeO_3$	0.55	0.584	0.566	0.556	0.567	0.537	0.562	Refs. 7 and 33	Ref. 34
$x(K_{0.5}Bi_{0.5})TiO_3$	0.15	0.131	0.169	0.188	0.188	0.225	0.225		
$yPbTiO_3$	0.3	0.285	0.265	0.256	0.245	0.238	0.213		
Crystal Structure	MPB	MPB	MPB	MPB	MPB	MPB	MPB	MPB	MPB
Tetragonality (c/a)	1.068	1.061	1.045	1.041	1.034	1.034	1.025	-	-
R_{WP} (%)	0.986	1.613	1.862	1.885	1.537	1.330	1.968	-	-
d_{33} (pm/V)	140	152	206	228	208	220	203	223	441
$-d_{31}$ (pm/V)	23.35	43.54	58.91	53.2	60.76	49.75	60.27	93.5	117
k_p	0.16	0.31	0.39	0.29	0.39	0.29	0.40	0.313	0.58
E_C (kV/mm)	5.99	4.21	3.93	3.64	3.82	3.98	4.01	-	-
T_C (°C)	542	514	442	427	422	419	410	386	447
T_d (°C)	523	489	416	409	390	380	395	~200	~400

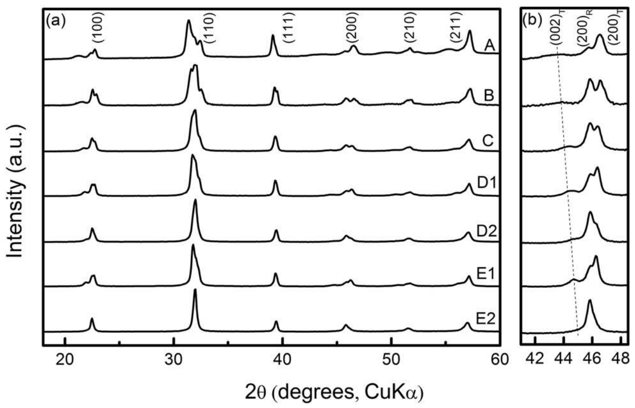

FIG. 2. (a) X-ray diffraction patterns of BF-KBT-PT ceramics in the 2θ range of 18°–60° and (b) from 41° to 48.5°.

piezoelectric properties as in lanthanum doped BFPT[20] and the discourse follows this position.

An example of the permittivity as a function of temperature has been included to exemplify the results. A reduction in $PbTiO_3$ content leads to a drop in the T_C. The highest T_C found was 542 °C in composition A which has the highest $PbTiO_3$ concentration. The dielectric loss is also shown in Fig. 3(a), the transition generally becoming more diffuse with reduced $PbTiO_3$ in agreement with the permittivity data. Impedance analysis as a function of temperature, shown in Figure 3(b), was used to further probe the potential operating temperatures of this system. The k_p of these materials was found to range from 0.16 to 0.4 at room temperature and this was relatively stable in all materials until the onset of depolarization. The same behaviour was observed in d_{31} values, although with much greater temperature dependence as anticipated due to the association with permittivity as a function of temperature. Values at room temperature were in the region of −23.35 pm/V to −60.76 pm/V, this reached as high as −188.9 pm/V at 320 °C in composition E2.

Despite the large tetragonality in selected compositions, the fabrication of dense sintered ceramics was achieved which is not always possible such as in BFPT or $PbTiO_3$ where this is particularly problematic and appropriate processing is required, notably slow cooling rates through the paraelectric phase transition. The addition of KBT in BFPT resulted in the migration of the MPB which occurs at ca. 70% $BiFeO_3$ to lower lead-titanate concentrations. Such a shift is observed in other mixed phase systems, or as a result of doping. The lattice parameters and c/a ratio are shown in Figure 4(a), the *a*-lattice parameter does not change significantly with increased $PbTiO_3$ content in contrast to the *c*-lattice parameter. Figure 4(b) shows the relationship between the $PbTiO_3$ content and the Curie temperature and room temperature piezoelectric d_{33}. The correlation between the lattice distortion and the Curie temperature has been widely discussed in La-doped BFPT piezoelectric ceramics,[20] here we show that an increase in room temperature spontaneous strain is coupled with an increased Curie temperature which is consistent with the thermodynamic models of ferroelectricity.[31] This is of note in the BFPT system where the c/a ratio is found to be 1.18 at the MPB where La-doping leads to significant reduction in the c/a ratio and a threshold c/a ratio was identified at 1.045, above which the coercive field is elevated and limited domain switching occurs. In agreement with the literature, the BF-KBT-PT system exhibits a reduction in electrical properties with an enhancement in the Curie temperature above a threshold c/a ratio, as evidenced by compositions A and B which exhibit c/a ratios in excess of 1.045 and much reduced room temperature d_{33} values. The highest c/a ratio of the compositions was 1.068 with a corresponding T_C of 542 °C, and d_{33} of 140 pm/V.

With decreasing $PbTiO_3$, significant peak broadening of the permittivity peaks occurred. It was accompanied with a shift in the T_C toward higher temperatures and the suppression of permittivity with increasing frequency, the origin of this is beyond the scope of this contribution. A reduction in $PbTiO_3$ leads to a general increase in room temperature permittivity and a decrease in T_C occurs as the energy barrier required to produce the paraelectric cubic phase is reduced. In terms of the piezoelectric coefficients, the T_d was commensurate with the T_C and no intermediate transitions were found between room temperature and the ferroelectric-paraelectric phase transition in contrast to a previous publication on this system which lied outside of the MPB region.[27]

The coercive field of these materials was determined using strain-field loops at 0.1 Hz with a maximum applied field of 7 kV/mm at room-temperature. As a family, the coercive field was observed to be much lower than the BFPT system and higher than the PZT system, allied with the

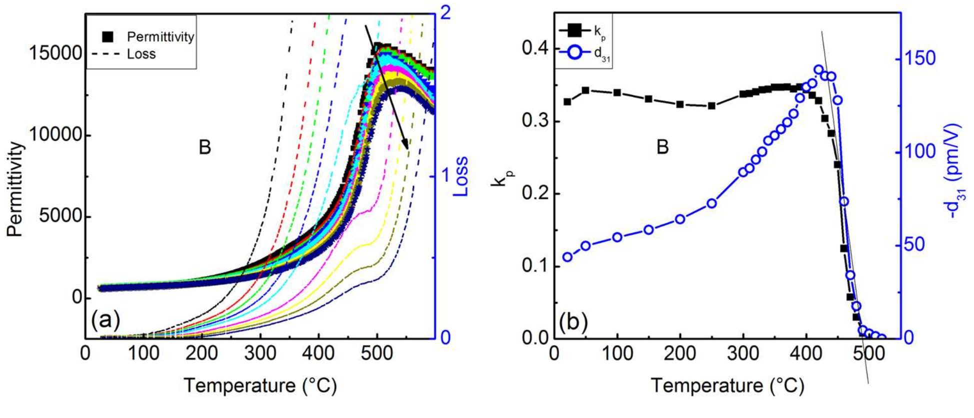

FIG. 3. Temperature dependence of (a) permittivity and loss and (b) of k_p and $-d_{31}$ for composition B.

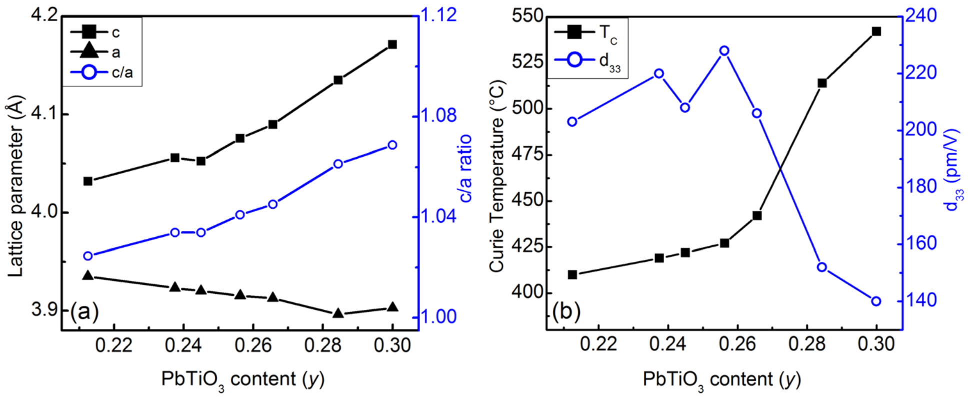

FIG. 4. (a) Lattice parameters and c/a ratio with varying $PbTiO_3$ content and (b) the relationship between the $PbTiO_3$ content and T_C & d_{33}.

respective c/a ratio and Curie temperature. Composition A with the highest coercive field did not exhibit fully saturated strain-field loops in contrast to the other compositions, which explains this unusually high value. Generally, a high c/a ratio and coercive field were also observed, this may lead to improved domain stability when subject to electrical fields. The low-field d_{33} was measured for each composition using a Berlincourt meter at 110 Hz and can be observed in Table I along with some of the key structural and electrical properties established during this investigation. Values of an unmodified PZT and BSPT have been included for comparison.

The operating window of this system coupled with respectable piezoelectric coefficients far exceeds any comparable materials as shown in Fig. 5, adapted from Zhangs review of high temperature sensors.[32] This figure contrasts relaxor-PT compositions, doped PZT, Mn-doped BSPT, BLSF, and perovskite layer structures with the compositions discussed in this contribution. The only materials which can rival compositions A and B are not classical perovskite structures and offer much reduced piezoelectric coefficients.

Samples of the (1-*x*-*y*)$BiFeO_3$-*x*$(K_{0.5}Bi_{0.5})TiO_3$-$_y$$PbTiO_3$ ternary solid solution were fabricated using the conventional solid-state reaction method. An MPB was observed between rhombohedral and tetragonal symmetry using XRD across a broad range of compositions. The depolarisation temperature was commensurate with the Curie temperature. High temperature stability is recorded for k_p until 50–100 °C below T_C. The highest temperature member of this family exhibits a $T_C = 542\,°C$, with a $d_{33} = 140$ pm/V; this is considerably higher than any other material with a similar T_C. This high temperature system has been developed without the use of prohibitively expensive Sc_2O_3, and with an operating ceiling in excess of PZT. The T_c and tetragonal spontaneous strain were identified to correlate strongly with the $PbTiO_3$ concentration, thus allowing tailoring of the structural and piezoelectric properties making this system an excellent candidate for use in high temperature piezoelectric applications.

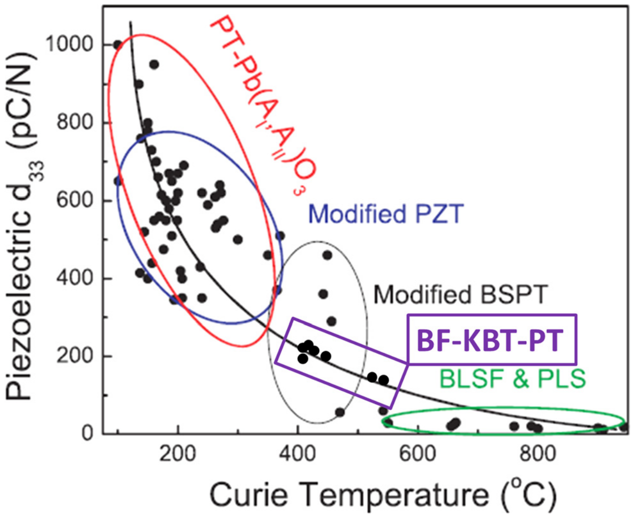

FIG. 5. d_{33} as a function of Curie temperature for a wide range of ceramics with the rectangle highlighting the BF-KBT-PT system. Reprinted with permission from S. Zhang and F. Yu, J. Am. Ceram. Soc. **94**(10), 3153 (2011). Copyright 2011 The American Ceramic Society.

This research has been supported by an EPSRC DTA (EP/P505593/1) and Ionix Advanced Technologies (www.ionix.at).

[1] R. C. Turner, P. A. Fuierer, R. E. Newnham, and T. R. Shrout, Applied Acoust. **41**(4), 299 (1994).
[2] C. A. Randall, A. Kelnberger, G. Y. Yang, R. E. Eitel, and T. R. Shrout, J. Electroceram. **14**(3), 177 (2005).
[3] D. Damjanovic, Curr. Opin. Solid State Mater. Sci. **3**(5), 469 (1998).
[4] R. E. Eitel, C. A. Randall, T. R. Shrout, and S. E. Park, Jpn. J. Appl. Phys., Part 1 **41**(4A), 2099 (2002).
[5] G. Shirane and A. Takeda, J. Phys. Soc. Jpn. **7**(1), 5 (1952).
[6] E.-M. Anton, W. Jo, D. Damjanovic, and J. Rodel, J. Appl. Phys. **110**(9), 094108 (2011).
[7] B. Jaffe and W. R. Cook, *Piezoelectric Ceramics* (Academic Press, London, 1971).
[8] S. Zhang, R. Xia, C. A. Randall, T. R. Shrout, R. Duan, and R. F. Speyer, J. Mater. Res. **20**(8), 2067 (2005).
[9] S. Zhang, E. Alberta, R. E. Eitel, P. W. Rehrig, W. Hackenberger, C. A. Randall, and T. R. Shrout, Proc. SPIE **5761**, 279 (2005).
[10] W. W. Wolny, J. Eur. Ceram. Soc. **25**(12), 1971 (2005).
[11] P. Hu, J. Chen, Z. Yu, L. Zhou, J. Deng, and X. Xing, J. Mater. Chem. **22**(13), 6311 (2012).
[12] W. Hu, X. Tan, and K. Rajan, J. Eur. Ceram. Soc. **31**(5), 801 (2011).
[13] T. Sebastian, I. Sterianou, D. Sinclair, A. J. Bell, D. A. Hall, and I. Reaney, J. Electroceram. **25**(2), 130 (2010).
[14] D. M. Stein and P. K. Davies, Appl. Phys. Lett. **99**(18), 182907 (2011).
[15] D. M. Stein, I. Grinberg, A. M. Rappe, and P. K. Davies, J. Appl. Phys. **110**(7), 074110 (2011).
[16] S. A. Fedulov, P. B. Ladyzhinskii, I. L. Pyatigorskaya, and Y. N. Venevtsev, Sov. Phys. Solid State **6**(2), 375 (1964).
[17] V. V. S. S. Sai Sunder, A. Halliyal, and A. M. Umarji, J. Mater. Res. **10**, 1301 (1995).
[18] T. Stevenson, T. P. Comyn, A. Daoud-Aladine, and A. J. Bell, J. Magn. Magn. Mater. **322**(22), L64 (2010).
[19] T. P. Comyn, T. Stevenson, and A. J. Bell, J. Phys. IV **128**, 13 (2005).
[20] T. Leist, T. Granzow, W. Jo, and J. Rodel, J. Appl. Phys. **108**(1), 014103 (2010).

[21] J. M. Kim, Y. S. Sung, J. H. Cho, T. K. Song, M. H. Kim, H. H. Chong, T. G. Park, D. Do, and S. S. Kim, Ferroelectrics **404**, 88 (2010).

[22] H. Matsuo, Y. Noguchi, M. Miyayama, M. Suzuki, A. Watanabe, S. Sasabe, T. Ozaki, S. Mori, S. Torii, and T. Kamiyama, J. Appl. Phys. **108**(10), 104103 (2010).

[23] T. Ozaki, H. Matsuo, Y. Noguchi, M. Miyayama, and S. Mori, Jpn. J. Appl. Phys. Part 1 **49**(9), 09MC05 (2010).

[24] M. I. Morozov, M. A. Einarsrud, and T. Grande, Appl. Phys. Lett. **101**(25), 252904 (2012).

[25] M. I. Morozov, M. A. Einarsrud, T. Grande, and D. Damjanovic, Ferroelectrics **439**(1), 88 (2012).

[26] J. Bennett, A. J. Bell, T. J. Stevenson, R. I. Smith, I. Sterianou, I. M. Reaney, and T. P. Comyn, Mater. Lett. **94**, 172 (2013).

[27] J. Bennett, A. J. Bell, T. J. Stevenson, and T. P. Comyn, Scr. Mater. **68**(7), 491 (2013).

[28] V. K. Seth, G. J. Gatins, and W. A. Schulze, Ferroelectrics **87**(1), 243 (1988).

[29] ANSI/IEEE Std 176-1987 (1988).

[30] Y. Hiruma, H. Nagata, and T. Takenaka, J. Appl. Phys. **105**(8), 084112 (2009).

[31] A. F. Devonshire, Adv. Phys. **3**(10), 85 (1954).

[32] S. Zhang and F. Yu, J. Am. Ceram. Soc. **94**(10), 3153 (2011).

[33] D. A. Berlincourt, C. Cmolik, and H. Jaffe, Proceedings of the IRE **48**(2), 220 (1960).

[34] J. Chen, H. Shi, G. Liu, J. R. Cheng, and S. Dong, J. Alloys Compd. **537**, 280 (2012).